RSC Advances

PAPER

View Article Online
View Journal | View Issue

Cite this: *RSC Adv.*, 2025, **15**, 39223

Biophysical and structural modifications on human erythrocytes induced by ethanolic extracts of *Ruta graveolens*, *Artemisia ludoviciana*, and *Lippia graveolens*: a study by ATR-FTIR spectroscopy

Emmanuel de la O-Cuevas, *[ab] P. Gallegos-Flores,[b] J. J. Ortega-Sigala,[b] H. Tototzintle-Huitle,[b] José M. Saniger[c] and E. L. Esparza-Ibarra*[a]

By using ATR-FTIR spectroscopy and spectral deconvolution analysis, biophysical and structural modifications induced by ethanolic extracts of *Rutta graveolens*, *Artemisia ludoviciana*, and *Lippia graveolens* (commonly used as medicinal plants) on human erythrocytes were investigated. The extracts were directly applied to the human erythrocytes. Their effects were analysed in relevant spectral regions, including the lipid and phospholipid vibration region (3010–2800 cm^{-1}), the carbonyl (C=O) stretching region (1770–1700 cm^{-1}), and the protein regions corresponding to amide I and amide II bands (1700–1600 cm^{-1} and 1600–1450 cm^{-1}, respectively). The ATR-FTIR characterization of the extracts revealed molecular vibrations associated with the presence of monoterpenes and flavonoids in *Ruta graveolens*, sesquiterpene lactones and phenolic compounds in *Artemisia ludoviciana*, as well as phenolic monoterpenes as thymol and carvacrol in *Lippia graveolens*. Spectral deconvolution analysis revealed shifts and increased intensities in absorption bands, indicating a loss of secondary structures and disruption of the lipid bilayer, as well as conformational rearrangements in proteins. Notably, alterations were observed in the relative proportions of α-helices, β-sheets, and disordered structures. The results obtained through ATR-FTIR spectroscopy and spectral deconvolution analysis provide biophysical evidence that largely elucidates the interactions and effects exerted by the plant extracts on human erythrocytes.

Received 29th August 2025
Accepted 7th October 2025

DOI: 10.1039/d5ra06459g

rsc.li/rsc-advances

1. Introduction

Throughout history, most cultures have relied on plants as their primary source of healthcare, making them an essential part of their traditional medical practices. According to the World Health Organization (WHO), approximately 80% of the global population use traditional medicine to meet their primary healthcare needs.[1–3] This widespread use has sparked growing scientific interest in validating and understanding the biochemical mechanisms behind these practices, supporting the use of these biological resources as valuable sources for identifying and developing new bioactive compounds suitable for both pharmacological and biomedical applications.[4–7]

Traditional medicine in Mexico plays and important role as a complementary pharmacological source for healthcare.[8–10] *Ruta graveolens*, *Lippia graveolens*, and *Artemisia ludoviciana* are species that have been used to treat various conditions and diseases, including gastrointestinal disorders, colic, infections, inflammation, and menstrual cycle disorders, among others. To understand and justify their use, several studies have reported that the phytochemical profiles of these species are characterized by the presence of secondary metabolites such as flavonoids, alkaloids, tannins, terpenoids, phenolic compounds, and essential oils, which are believed to be responsible for the pharmacological effects that have been reported for these plants.[11–16]

The use of these plants is based on ethnomedical evidence; however, few studies have methodically analysed their effects on human cells, specifically with possible structural alterations at the cellular level. For this reason, human erythrocytes, or red blood cells, may be a suitable cellular model for evaluating the biocompatibility of these natural compounds.[17,18] Erythrocytes are characterized by their relative structural simplicity, as they lack a nucleus and organelles, as well as their easy accessibility and abundance. Therefore, erythrocytes allow for adequate analysis of the physical and chemical modifications that can be induced in their cell membrane.[19,20] The cell membrane

[a]*Unidad Académica de Ciencias Biológicas, Universidad Autónoma de Zacatecas, 98068, Zacatecas, Mexico. E-mail: emmanuel.delao@fisica.uaz.edu.mx; lesparza@uaz.edu.mx*

[b]*Unidad Académica de Física, Universidad Autónoma de Zacatecas, 98068, Zacatecas, Mexico*

[c]*Instituto de Ciencias Aplicadas y Tecnología, Universidad Nacional Autónoma de México, Circuito exterior S/N, Ciudad Universitaria, 04510, Ciudad de Mexico*

consists of a highly dynamic lipid bilayer, glycoconjugates, and structural proteins, the integrity of which is essential for cell functionality. However, it has been reported that haemolysis processes, membrane stiffness, oxidative stress, or protein denaturation are due to alterations in the composition and structure of the cell membrane,[21–23] which justifies the study of the exposure of human erythrocytes to plant extracts, as they can be a sensitive tool for detecting and monitoring possible alterations (adverse or protective) caused by interaction with the various secondary metabolites present in plants.

To study the interactions between secondary metabolites and human erythrocytes, Fourier-transform infrared spectroscopy (FTIR) is the appropriate technique, as it provides physical, chemical, and structural information and is highly sensitive to changes in the microenvironment of the analysed sample. FTIR spectroscopy is based on the absorption of infrared electromagnetic radiation by the chemical bonds of molecules. This absorption provides vibrational spectra, or "fingerprints", characteristic of each molecule. Currently, FTIR spectroscopy has established itself as an effective technique for the molecular-level studies of biological systems, as it allows for the simultaneous and non-destructive analysis of both lipid components and protein secondary structures. In the case of human erythrocytes, it provides detailed information about the lipid bilayer as well as the structural proteins, while also enabling the identification of changes or alterations induced by the secondary metabolites of plant extracts.[24–29] FTIR spectroscopy offers numerous advantages; it is a non-invasive and non-destructive technique, requires minimal sample amounts, involves very short analysis times, and can be combined with multivariate statistical methods such as principal component analysis (PCA), partial least squares regression (PLS), and others. Spectral deconvolution techniques can also be implemented. All these methods allow for the identification of subtle changes in the spectral profiles of the analysed samples. In the study of biological systems such as human erythrocytes, the spectral regions associated with aliphatic stretching of the methylene and methyl groups (3000–2800 cm^{-1}), as well as the amide I (1700–1600 cm^{-1}), and amide II (1580–1400 cm^{-1}) bands, provide key information on the lipid organisation and secondary conformation of membrane proteins. The sensitivity of these bands to structural changes makes FTIR spectroscopy an effective tool for evaluating the effects of metabolites present in plant extracts on biomolecules in erythrocytes.[24–29]

A way to track and identify these structural changes, which are not so obvious, is through spectral deconvolution, which is a signal processing technique that alloys for the recovery of the intrinsic spectral information of a sample. By applying mathematical deconvolution algorithms, it is possible to obtain spectra with a resolution higher that the instrument's nominal resolution, revealing spectral details that would otherwise remain hidden or misidentified. The information provided by spectral deconvolution enables the precise location of bands, widths, and intensities, and facilitates the identification and separation of multispectral components, as well as the detection of weak signals masked by instrumental noise, thereby increasing the analysis capacity when compared to direct analysis of the original spectrum.[30–37]

Despite the growing use of FTIR spectroscopy in biomedical studies, few investigations employ this technique to characterize the interactions between ethanolic extracts of medicinal plants and human erythrocytes. Therefore, it is important to incorporate this spectroscopic technique to study, from a biophysical approach, the impact of these natural compounds on blood cells. In this context, the present study aims to analyse and characterize, using ATR-FTIR spectroscopy and spectral deconvolution, the possible modifications induced on lipid bilayer and structural membrane proteins caused by ethanolic extracts of *Ruta graveolens*, *Artemisia ludoviciana*, and *Lippia graveolens*.

2. Experimental

2.1 Preparation of ethanolic extracts from shrub plants

As plant material, stems, leaves, and flowers of the shrub species were used: *Ruta graveolens*, *Artemisia ludoviciana*, *and Lippia graveolens*. The plants were collected during October 2023 in the municipalities of General Pánfilo Natera and Valparaíso, in the state of Zacatecas, México. 500 g of fresh plant material per species was obtained, which was washed with distilled water to eliminate impurities and solid particles. Subsequently, excess water was removed with absorbent paper, and the samples were dehydrated in a Thermo Scientific oven at 45 °C for 48 hours. Once dry, the samples were pulverized in a mortar to obtain a fine powder.

The ethanolic extraction was carried out using a ratio of 25 g of dry plant material per 200 mL of 96% ethanol (v/v). The mixture was placed in amber bottles and macerated for 30 days, with mechanical agitation every three days. At the end of the process, the extract was filtered using filter paper with a pore size of 8 μm. The concentrated ethanolic extract was stored in amber bottles, labelled, and kept at room temperature (20–25 °C) until further analysis.

2.2 Human erythrocytes cell lysis assay

5 mL of type O Rh-positive human blood was obtained by venous puncture, collected in BD Vacutainer tubes with sodium citrate as an anticoagulant. The sample was centrifuged at 2500 rpm for 7 minutes at room temperature to separate the plasma, which was carefully removed. The remaining packed cells were washed three times with 0.9% isotonic saline solution (NaCl), centrifuging at 2500 rpm for 5 minutes in each wash. The recovered erythrocytes were prepared in a 3% (v/v) suspension in physiological solution.

The treatment with extracts, 500 μL of the 3% erythrocytes suspension was mixed with 500 μL of each ethanolic extract (*Ruta graveolens*, *Artemisia ludoviciana*, and *Lippia graveolens*) in 1.5 mL Eppendorf tubes. The samples were incubated for 3 hours at room temperature. After this period, the tubes were centrifuged at 8500 rpm for 5 minutes, the supernatant was removed, and the precipitate with cell debris was recovered. From this precipitate, 5 μL were placed on aluminium plates,

which were left to dry for 30 minutes in an atmosphere at 25% relative humidity and at room temperature, for subsequent analysis by FTIR spectroscopy.

Likewise, two controls were used; the negative control consisted of the mixture of 500 μL of 3% erythrocytes with 500 μL of physiological solution; the positive control was prepared by mixing 500 μL of 3% erythrocytes with 500 μL of 1% Triton X-100 to induce complete lysis. The ATR-FTIR spectra of the positive control are presented in the SI, Fig. S1.

This study was approved by the Institutional Ethics Committee of the Autonomous University of Zacatecas and the Research Ethics Committee of the General Hospital of Zacatecas "Luz González Cosío", and carried out following the guidelines of the Helsinki Declaration. Informed consents were obtained from human participants of this study.

2.3 Fourier-transform infrared (FTIR) spectroscopy measurements

The Fourier-transform infrared (FTIR) spectroscopy analysis was performed on a Nicolet iS50 FTIR Thermo Scientific spectrometer, equipped with an attenuated total reflectance (ATR) accessory with a diamond crystal. Spectra acquisition was carried out with 32 scans, a spectral resolution of 4 cm^{-1}, in a spectral range of 600 cm^{-1} to 3600 cm^{-1}. The working spectrum for each sample corresponded to the average of 10 recorded spectra.

2.4 Deconvolution of ATR-FTIR spectra

Deconvolution of ATR-FTIR spectra was carried out using OriginPro 2024 software, employing a procedure designed to resolve overlapping bands and improve spectral interpretation. First, the spectral regions of interest were delimited: 3010–2800 cm^{-1}, 1770–1700 cm^{-1}, 1700–1600 cm^{-1}, and 1600–1450 cm^{-1}. To each of these regions, a Savitzky–Golay type smoothing was applied, with a 5-point window, to reduce noise without distorting the shape of the bands. Subsequently, a baseline correction was performed to eliminate non-spectroscopic contributions and facilitate the identification of real signals. The next step consisted of calculating the second derivative of the spectrum, which allowed estimating the number and approximate position of the bands within each region. Finally, a non-linear curve fitting was carried out using Gaussian functions, where the number and approximated bands position (control spectrum) was fixed for the analysis of each sample, allowing the separation and quantification of the individual bands that compose each signal.

3. Results and discussion

3.1 ATR-FTIR characterization of ethanolic extracts of *Ruta graveolens*, *Artemisia ludoviciana*, and *Lippia graveolens*

The ATR-FTIR spectra of ethanolic extracts of *Ruta graveolens*, *Artemisia ludoviciana*, and *Lippia graveolens* are shown in Fig. 1. Below, a detailed description of the vibrational modes observed in each spectrum is presented, along with their association with various functional groups related to the presence of secondary metabolites in the ethanolic extracts of these plant compounds.

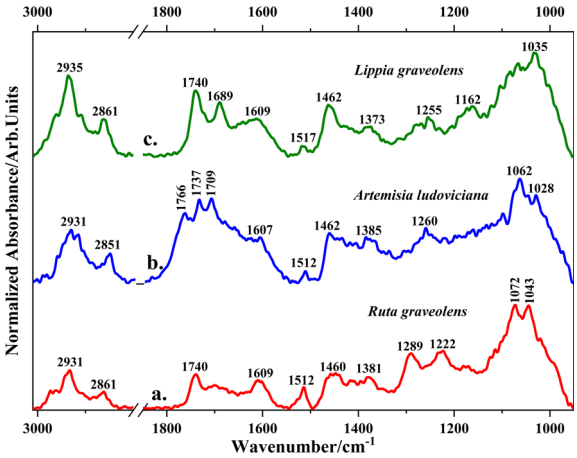

Fig. 1 ATR-FTIR spectra of ethanolic extracts of *Ruta graveolens* (a), *Artemisia ludoviciana* (b), and *Lippia graveolens* (c).

3.1.1 Ruta graveolens. In Fig. 1(a), the ATR-FTIR spectrum of the ethanolic extract of *Ruta graveolens* is shown, where bands centred at 2931 cm^{-1} and 2861 cm^{-1} are observed, which correspond to the asymmetric and symmetric stretching vibrations of the methylene groups (CH_2), commonly present in essential oils, waxes, and terpene metabolites. These bands are associated with the presence of monoterpenes such as limonene. Additionally, a band centred at 1740 cm^{-1} is observed, attributed to the stretching vibration of the carbonyl group (C=O), which can be associated with the presence of esters and methoxylated flavonoids. The bands centred at 1609 cm^{-1} and 1512 cm^{-1} are associated with C=C stretching vibrations in aromatic rings and with N–H bond bending, respectively, which suggests the presence of flavonoids and alkaloids with conjugated aromatic structures. Likewise, the bands centred at 1460 cm^{-1} and 1381 cm^{-1} correspond to deformation vibrational modes of the methyl (CH_3) and methylene (CH_2) groups, respectively, characteristic of branched hydrocarbon structures present in terpenes and phenolic compounds. The bands located at 1289 cm^{-1} and 1222 cm^{-1} can be attributed to C–O bond stretching vibrations, associated with esters and phenolic acids. Finally, the most intense bands observed at 1072 cm^{-1} and 1043 cm^{-1} are due to C–O and C–C stretching vibrations presents in carbohydrates.[11–14,38,39]

3.1.2 Artemisia ludoviciana. The ATR-FTIR spectrum (Fig. 1(b)) of the ethanolic extract of *Artemisia ludoviciana* shows bands centred at 2931 cm^{-1} and 2851 cm^{-1}, due to asymmetric and symmetric stretching vibrations of the methylene groups. These vibrational modes are related to the presence of terpene structures, including cineole, thujone, and borneol. The bands centred at 1766 cm^{-1}, 1737 cm^{-1}, and 1709 cm^{-1} are due to the stretching vibration of the carbonyl group (C=O), which, by the location of the bands, is associated with carbonyl groups in different chemical environments. Likewise, the bands centred at 1607 cm^{-1}, 1512 cm^{-1}, 1462 cm^{-1}, and 1385 cm^{-1} are due to vibrations of aromatic structures and deformations of the

methyl and methylene groups, which suggests the presence of phenolic compounds such as flavonoids and phenolic acids. On the other hand, the bands located at 1260 cm^{-1}, 1162 cm^{-1}, and 1062 cm^{-1} correspond to C–O and C–C bond stretching vibrations, originating from esters and glycosylated phenolic compounds. These results are consistent with previous phytochemical studies of *Artemisia ludoviciana*, in which a wide variety of secondary metabolites have been described, including flavonoids, sesquiterpene lactones, tannins, and essential oil components.[11–14,40]

3.1.3 Lippia graveolens. Fig. 1(c) shows the ATR-FTIR spectrum of the ethanolic extract of *Lippia graveolens*, where bands centred at 2935 cm^{-1} and 2861 cm^{-1} are observed, which correspond to asymmetric and symmetric stretching vibrations of the methylene groups, respectively. These bands reveal the presence of saturated aliphatic chains, in agreement with the presence of monoterpenes, such as thymol and carvacrol, which have been reported on this species. The band centred at 1740 cm^{-1} is due to the stretching vibration of the carbonyl group (C=O), corresponding to organic acid esters and esterified terpenoid compounds. The band centred at 1689 cm^{-1} is due to the stretching vibration of conjugated carbonyl groups, related to the presence of oxygenated flavonoids or quinones. The bands centred at 1609 cm^{-1}, 1517 cm^{-1}, 1462 cm^{-1}, and 1373 cm^{-1} are due to C=C stretching vibrations of aromatic structures and to deformations of the methyl and methylene groups; these vibrational modes are related to the presence of phenolic compounds, including flavonoids and phenolic acids. Additionally, the band centred at 1255 cm^{-1} can be attributed to C–O stretching vibrations of phenolic esters and glycosylated compounds. Finally, the bands centred at 1162 cm^{-1} and 1035 cm^{-1} correspond to C–O and C–C bond vibrations, characteristic of alcohols, phenols, and terpene structures, particularly associated with carvacrol and thymol, compounds found in the essential oil of *Lippia graveolens*.[11–14,41,42]

3.2 ATR-FTIR characterization of human erythrocytes treated with ethanolic extracts of *Ruta graveolens*, *Artemisia ludoviciana*, and *Lippia graveolens*

3.2.1 Human erythrocytes. In Fig. 2(a), the ATR-FTIR spectrum of untreated human erythrocytes (control) is presented, in which well-defined bands centred at 2965 cm^{-1}, 2936 cm^{-1}, and 2862 cm^{-1} are observed, corresponding to asymmetric and symmetric stretching vibrations of the methyl (CH_3) and methylene (CH_2) groups. These vibrational modes originate from the aliphatic hydrocarbon chains of the fatty acids that compose the lipid bilayer of the erythrocyte membrane. The intensity and location of these bands are associated with the abundance and organisation of phospholipids that constitute the structure of the cell membrane.[24–26,43–45]

The band centred at 1744 cm^{-1} is due to the stretching vibration of the carbonyl group (C=O) and is mainly attributed to the phospholipids that integrate the lipid bilayer of the erythrocyte membrane. This band originates from the carbonyl groups present in the esterified acyl chains of the glycerol backbone, a characteristic structure of membrane phospholipids. The location and intensity of this band reflect the conformational state and chemical integrity of these structural phospholipids.[24–26,43–45]

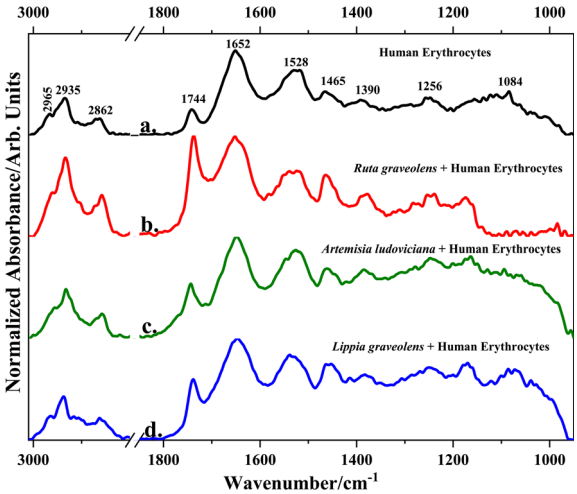

Fig. 2 ATR-FTIR spectra of untreated human erythrocytes (a), and human erythrocytes treated with ethanolic extracts of *Ruta graveolens* (b), *Artemisia ludoviciana* (c), and *Lippia graveolens* (d).

The band centred at 1652 cm^{-1} is characteristic of the stretching vibration of the carbonyl group (C=O) of the peptide bond in membrane proteins, and corresponds to the region called amide I. Meanwhile, the band centred at 1528 cm^{-1} corresponds to the region called amide II, which is associated with the combination of N–H bond bending vibrations and C–N bond stretching vibrations, also characteristic of the peptide backbone. These two bands are sensitive to conformational changes of proteins and provide information about their secondary structure. In particular, the location and intensity of these bands indicate a predominance of α-helix structures, which is consistent with the structure of haemoglobin, a cytoplasmic protein that represents approximately 95% of the total protein content of human erythrocytes.[24–26,43–45]

The bands centred at 1465 cm^{-1} and 1390 cm^{-1} are due to asymmetric deformation vibrations of the methyl groups and symmetric deformation vibrations of the methylene groups, respectively. These bands originate both in the amino acid side chains present in membrane proteins and in the fatty acids of the phospholipids that compose the lipid bilayer. Their location and intensity provide information about the conformation and organisation of the lipid and protein components of the erythrocyte membrane.[24–26,43–45]

The bands centred at 1256 cm^{-1} and 1084 cm^{-1} are attributed to stretching vibrations of the C–O bond and the phosphate group (PO_4^{3-}), respectively. These bands are associated with various molecular structures present in the erythrocyte membrane, including hydroxyl groups of membrane carbohydrates, ester bonds in phospholipids, as well as possible contributions from aromatic structure vibrations originating from amino acid residues present in haemoglobin. These bands provide information about the chemical composition and

functional environment of lipid and protein components.[24–26,43–45]

3.2.2 Human erythrocytes treated with *Ruta graveolens*, *Artemisia ludoviciana*, and *Lippia graveolens*. The ATR-FTIR spectrum shown in Fig. 2(b) reveals notable spectral modifications after treating human erythrocytes with the ethanolic extract of *Ruta graveolens*, which suggests significant interactions between the secondary metabolites present in the extract and the structural components of the erythrocyte membrane. Upon initial visual inspection, an increase in the intensity of the bands centred at 2925 cm^{-1}, 2862 cm^{-1}, and 1744 cm^{-1} is observed, corresponding to stretching vibrations of the methyl (CH_3), methylene (CH_2), and carbonyl (C=O) groups, respectively. This increase in intensity suggests a direct interaction with the fatty acids and phospholipids that form the lipid bilayer. On the other hand, in the amide I (1652 cm^{-1}) and amide II (1528 cm^{-1}) bands, some alterations in the spectral profiles are observed, which include variations in relative intensity, appearance of shoulders, and broadening of these bands, which can be attributed to possible modifications in the secondary structure of proteins. Additionally, in the bands centred at 1465 cm^{-1} and 1390 cm^{-1}, associated with deformation vibrations of the methyl and methylene groups, an increase in their intensities, compared with the control spectrum, is observed, which may be related to a reorganisation in the hydrocarbon side chain of lipids and proteins. Finally, marked alterations are observed in the bands centred at 1256 cm^{-1} and 1084 cm^{-1}, corresponding to C–O vibrations and phosphate groups, respectively. These spectral changes could indicate a modification in membrane carbohydrates and in the polar domains of phospholipids, suggesting a deeper interaction with the hydrophilic portion of the lipid bilayer.[43–48]

In the case of erythrocytes treated with ethanolic extract of *Artemisia ludoviciana* (Fig. 2(c)) visual analysis of the ATR-FTIR spectrum shows evident spectral alterations, although less pronounced compared to those induced by *Ruta graveolens*. The bands centred at 2935 cm^{-1}, 2862 cm^{-1}, and 1744 cm^{-1} show a slight increase in their intensity, accompanied by notable broadening, which suggests interactions with the components of the lipid bilayer. In the amide I and amide II bands, changes in the spectral profiles are observed, manifested in the appearance of shoulders and variations in the relative intensity between both bands. These alterations could reflect changes in the secondary conformation of membrane proteins. Likewise, the bands centred at 1465 cm^{-1} and 1390 cm^{-1}, associated with deformation vibrations of the methyl and methylene groups, present a slightly broadened spectral profile, also showing the appearance of shoulders along with a slight increase in intensity and a shift toward lower wave numbers compared to the erythrocyte control spectrum. Finally, alterations are identified in the bands centred at 1256 cm^{-1} and 1084 cm^{-1}, corresponding to C–O stretching vibrations and the phosphate group, respectively, which suggests possible interactions with membrane carbohydrates and with the polar region of phospholipids.[43–48]

On the other hand, in the ATR-FTIR spectrum of human erythrocytes treated with the ethanolic extract of *Lippia graveolens* presented in Fig. 2(d), some spectral changes compared with the control are observed. In the region between 3000 cm^{-1} and 2800 cm^{-1}, corresponding to stretching vibrations of methyl and methylene groups, a notable increase in the intensity of the bands is not observed; however, a broadening of them is detected, which suggests a possible reorganisation in the aliphatic chains of membrane lipids. The band centred at 1744 cm^{-1}, attributed to the stretching vibration of the carbonyl group (C=O), presents an increase in intensity and broadening, which indicates a possible interaction with the ester groups of the phospholipids of the lipid bilayer. In the region associated with proteins, amide I and amide II bands, changes in their relative intensities are observed, as well as broadening of these, which could indicate conformational changes in membrane proteins. Likewise, the bands centred at 1465 cm^{-1} and 1390 cm^{-1}, show an increase in their intensity, along with broadening, which suggests possible perturbations in the lipid and protein components. Finally, the bands centred at 1256 cm^{-1} and 1084 cm^{-1} present evident alterations compared to the control, which suggests interactions with phosphate groups and carbohydrates associated with the surface of the erythrocyte membrane.[43–48]

Visual inspection of ATR-FTIR spectra reveals alterations in human erythrocytes after treatment with different ethanolic extracts. However, to identify with great precision the molecular modification and interactions induced by the secondary metabolites, a more detailed analysis of the spectral regions of interest is necessary through spectral deconvolution techniques. As has been mentioned previously, spectral deconvolution allows the location of overlapping bands, facilitating the identification of individual spectral components that could remain masked in the original spectrum. The application of spectral deconvolution contributed significantly to the detection of subtle intensity changes, band shifts, as well as the appearance or disappearance of bands, which provides detailed information about alterations in specific functional groups. Consequently, this analysis allows a more rigorous and precise characterization of the interaction mechanisms between the bioactive components of plant extracts and the molecular structures of the erythrocyte membrane.

3.3 Spectral region analysis of ATR-FTIR spectra of human erythrocytes treated with ethanolic extracts of *Ruta graveolens*, *Artemisia ludoviciana*, and *Lippia graveolens*

3.3.1 Spectral region from 3000 cm^{-1} to 2800 cm^{-1}. In Fig. 3(a), the ATR-FTIR spectra corresponding to untreated human erythrocytes (control) and erythrocytes treated with ethanolic extracts of *Ruta graveolens*, *Artemisia ludoviciana*, and *Lippia graveolens* in the spectral region from 3000 cm^{-1} to 2800 cm^{-1} are presented. In this region, the asymmetric and symmetric stretching vibrations of the methylene and methyl groups are presented, attributed to the aliphatic chains of the fatty acids of the phospholipids that constitute the structure of the lipid bilayer. Modifications in the shape, intensity, or position of these bands have been associated with alterations in lipid order, fluidity, rigidity, and dynamics of the lipid bilayer.

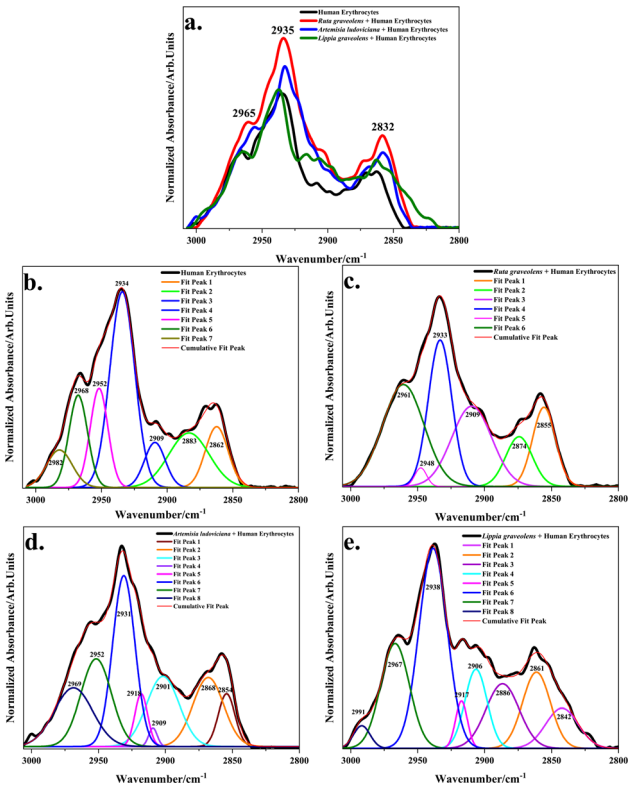

Fig. 3 ATR-FTIR spectra (3010–2800 cm^{-1}) of: (a) human erythrocytes and human erythrocytes treated with ethanolic extracts of *Ruta graveolens*, *Artemisia ludoviciana*, and *Lippia graveolens*, and (b–e) spectral deconvolution of each sample.

These alterations can be modified or altered by bioactive compounds and variations in the cellular microenvironment. The bands (control) centred at 2965 cm^{-1}, 2935 cm^{-1}, and 2862 cm^{-1}, which are characteristic of an ordered and functional lipid membrane in native state, experience notable changes in their intensity, shift and spectral profile after exposure to plant extracts, which suggests that interactions are being generated between the secondary metabolites present in the extracts and the lipid components of the membrane.[43–48]

Therefor, to understand in detail the changes observed in the spectral region of 3010–2800 cm^{-1}, Fig. 3(b) shows the spectral deconvolution of the ATR-FTIR spectrum of untreated human erythrocytes (control). Seven bands centred at 2982, 2968, 2952, 2934, 2909, 2883, and 2862 cm^{-1} are observed. The location of these is associated with specific vibrational modes of the methyl and methylene groups of the aliphatic chains of the phospholipids and reflects an ordered lipid system. The organisation and spectral distribution are associated with an erythrocyte membrane under normal conditions.[43–48]

On the other hand, Fig. 3(c) shows the spectral deconvolution of human erythrocytes treated with the ethanolic extract of *Ruta graveolens*. In this spectrum, six bands centred at 2987, 2962, 2948, 2933, 2909, and 2855 cm^{-1} are observed. A reduction in the number of spectral components and shift of several bands toward lower wave numbers is observed. These changes indicate a loss of order in the aliphatic chains of the phospholipids, which may suggest an increase in conformational flexibility and the freedom of movement of the methyl and methylene groups. These greater molecular dynamics may be associated with a decrease in the interaction between lipid chains, reflecting a less compact state of the lipid bilayer.[11,12,27–29,38,39,43–48]

Likewise, in Fig. 3(d), the spectral deconvolution of human erythrocytes treated with the ethanolic extract of *Artemisia ludoviciana* is shown, where eight bands centred at 2969, 2952, 2931, 2918, 2909, 2901, 2968, and 2854 cm^{-1} are observed. Compared to the control spectrum, the appearance of two new bands centred at 2918 cm^{-1} and 2901 cm^{-1} is observed, which suggests the presence of additional vibrational modes induced by modifications in the molecular organisation of the lipid bilayer. These changes could be related to the formation of microenvironments within the membrane, promoted by the interactions of secondary metabolites present in *Artemisia ludoviciana* with the lipid components. The observed spectral complexity indicates that the plant extract could be inducing local structural reorganisations that affect the dynamics and order of the phospholipids.[11,12,27–29,40,43–48]

Finally, Fig. 3(e) shows the spectral deconvolution of human erythrocytes treated with the ethanolic extract of *Lippia graveolens*, in which eight bands centred at 2991, 2967, 2938, 2917, 2909, 2886, 2861, and 2842 cm^{-1} are appreciated. Compared to the control spectrum, the appearance of three new bands centred at 2992 cm^{-1}, 2967 cm^{-1}, and 2842 cm^{-1} is observed, as well as a shift toward higher wavenumbers in several bands. The presence of these new bands indicates a significant restructuring of the lipid environment, while the observed shifts suggest the coexistence of different molecular conformations within the lipid bilayer. This spectral behaviour could be related to differentiated and simultaneous interactions between the secondary metabolites of the extract and specific regions of the membrane, which reflects a profound alteration in the organisation and dynamics of the lipid system.[11,12,27–29,41–48]

3.3.2 Spectral region from 1770 cm^{-1} to 1700 cm^{-1}. Fig. 4(a) shows the ATR-FTIR spectra of untreated human erythrocytes and those treated with ethanolic extracts of *Ruta graveolens*, *Artemisia ludoviciana*, and *Lippia graveolens*, in the spectral region associated with stretching vibrations of the carbonyl group (C=O) present in the phospholipids that form the lipid bilayer of the erythrocyte membrane. This region is highly sensitive for evaluating structural alterations induced by interactions with bioactive compounds. In all cases, an increase in band intensity is observed, which may be related to an increase in local rigidity of the lipid domains. This suggests that some secondary metabolites, such as flavonoids, terpenes, and phenolic compounds, could insert between the acyl chains of the phospholipids or interact with their polar heads, promoting spectroscopically detectable conformational modifications. Likewise, a shift of the band toward lower wavenumbers is appreciated, which indicates a reduction in the vibrational energy of the carbonyl group. This shift can be attributed to the formation of hydrogen bonds between the C=O groups of the phospholipids and the hydroxyl groups of the phenolic compounds present in the extracts.[27–29,31,32,45–49]

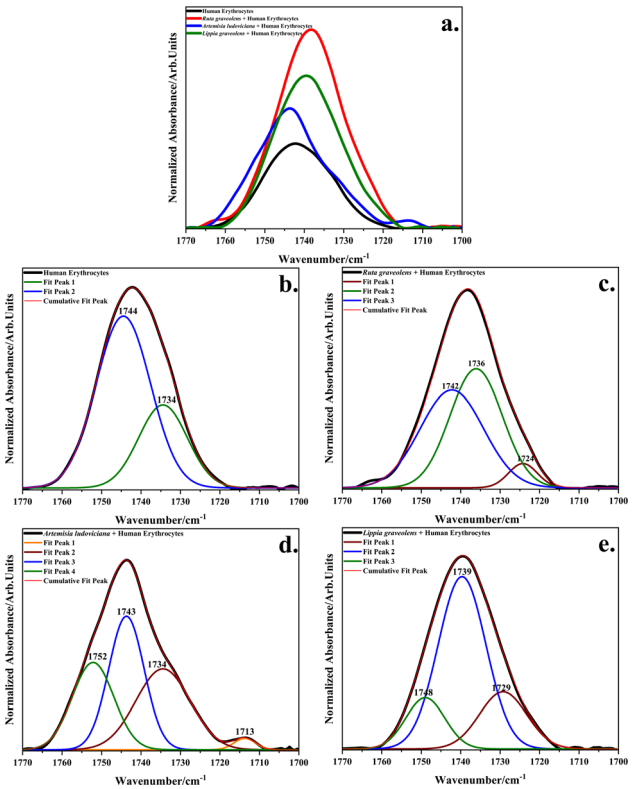

Fig. 4 ATR-FTIR spectra (1770–1700 cm^{-1}) of: (a) human erythrocytes and human erythrocytes treated with ethanolic extracts of *Ruta graveolens*, *Artemisia ludoviciana*, and *Lippia graveolens*, and (b–e) spectral deconvolution of each sample.

Fig. 4(b) shows the spectral deconvolution of the ATR-FTIR spectrum of untreated human erythrocytes (control), where two bands centred at 1744 cm^{-1} and 1734 cm^{-1} are observed. The band centred at 1744 cm^{-1} originates from esterified carbonyl vibrations located in more polar regions of the lipid bilayer, probably less affected by intermolecular interactions, such as hydrogen bonds. On the other hand, the band centred at 1734 cm^{-1} may correspond to carbonyls more exposed to the aqueous phase or partially hydrated. The presence of both bands suggests a heterogeneous distribution of carbonyl groups associated with the functional and dynamic structure of the membrane under native conditions.[27–29,31,32,45–49]

Fig. 4(c) presents the spectral deconvolution of human erythrocytes treated with *Ruta graveolens*, in which notable modifications in the shape, position, and intensity of the bands are observed compared to the control spectrum. Three bands centred at 1742 cm^{-1}, 1736 cm^{-1}, and 1742 cm^{-1} are observed. The slight shift of the main band from 1744 cm^{-1} to 1742 cm^{-1} may be due to superficial interactions of the van der Waals or dipole–dipole type with metabolites present in the extract. The appearance of the band at 1736 cm^{-1} indicates a greater proportion of carbonyls partially exposed to more polar environments, which suggests a reorganisation of the lipid environment. On the other hand, the band centred at 1724 cm^{-1} may be related to the formation of stronger hydrogen bonds between the carbonyl groups of the phospholipids and the hydroxyl groups of phenolic compounds present in *Ruta graveolens*, according to literature such as rutin, quercetin, or coumarin derivatives.[11,38,39] The location of this band at lower wavenumbers indicates a more stable interaction, which could induce relevant structural alterations in the lipid bilayer, such as the generation of more rigid domains or the formation of microenvironments with different degrees of lipid ordering.[11,12,27–29,31,32,45–49]

Fig. 4(d) shows the spectral deconvolution of the ATR-FTIR spectrum of human erythrocytes treated with the ethanolic extract of *Artemisia ludoviciana*, in which four bands centred at 1752 cm^{-1}, 1743 cm^{-1}, 1734 cm^{-1}, and 1713 cm^{-1} are observed. The presence of the band at 1752 cm^{-1} is associated with a state of low intermolecular interaction. This phenomenon could be due to greater exposure of carbonyls to a polar environment, possibly induced by bioactive compounds present in the extract, such as sesquiterpenes and volatile components of essential oils. These metabolites could disorganize the hydrophilic interactions at the lipid–water interface, altering the microenvironment of the lipid bilayer. In turn, the bands centred at 1743 cm^{-1} and 1734 cm^{-1}, exhibit an increase in their relative intensity, which could indicate a redistribution of the immediate polar environment of the carbonyls of the phospholipids. This redistribution suggests the interaction or insertion of polar metabolites with specific regions of the bilayer, without causing significant energetic shifts. Finally, the appearance of the band centred at 1713 cm^{-1} could be due to the formation of particularly strong hydrogen bonds, possible derived from interactions between carbonyl groups and phenolic compounds such as flavonoids. This type of interaction can facilitate the anchoring of secondary metabolites in specific domains of the membrane, promoting a lipid microenvironment of different polarity and structural order.[11,12,27–29,31,32,45–49]

Finally, Fig. 4(e) presents the spectral deconvolution of human erythrocytes treated with the ethanolic extract of *Lippia graveolens*, where three bands centred at 1739 cm^{-1}, 1729 cm^{-1}, and 1718 cm^{-1} are observed. The shift of the band observed in the control (1744 cm^{-1}) toward lower wavenumbers (1739 cm^{-1}) suggests a slight alteration in the microenvironment of the less polar carbonyl groups, possibly due to low-energy interactions such as dipole–dipole or van der Waals interactions. The bands centred at 1729 cm^{-1} and 1718 cm^{-1} indicate greater participation of the carbonyls in hydrogen bonds, possibly with hydroxyl groups of phenolic compounds reported for this extract.[11,41,42] This interaction can promote a reorganisation of the lipid environment, favouring greater structural order without compromising the general fluidity of the membrane. The symmetry and definition of the observed bands suggest a redistribution of interaction sites and a structural integration compatible with the functional stability of the erythrocyte membrane.[11,12,27–29,31,32,45–49]

3.3.3 Spectral region from 1700 cm^{-1} to 1600 cm^{-1}. The spectral region between 1700 cm^{-1} and 1600 cm^{-1}, the amide I region, is sensitive to changes in the secondary structures of proteins. This region originates mainly from the stretching vibration of the carbonyl group (C=O) of the peptide backbone, and its spectral profile provides information about the

secondary conformation of proteins, which is related to α-helix, β-sheets, β-turns, and disordered structures. The relative proportion and distribution of these structures can be altered by variations in the microenvironment, interaction with bioactive compounds, or chemical stress conditions. In this context, the comparative analysis of ATR-FTIR spectra and their spectral deconvolution analysis allows evaluating with high sensitivity the possible conformational modifications induced by the ethanolic extracts of *Ruta graveolens*, *Artemisia ludoviciana*, and *Lippia graveolens* on the membrane proteins present in human erythrocytes. This spectroscopic approach contributes to the understanding of the biophysical and molecular effects that these natural metabolites can exert on the protein structure of the cell membrane.

Fig. 5(a) shows the ATR-FTIR spectra of untreated human erythrocytes and those treated with ethanolic extracts of *Ruta graveolens*, *Artemisia ludoviciana*, and *Lippia graveolens*, in the amide I spectral region. A general decrease in absorption intensity is observed after treatment with the extracts, compared to the control spectrum. This reduction in intensity can be interpreted as an indication of partial loss of ordered secondary structure of proteins, or of a conformational reorganisation induced by interaction with metabolites present in the extracts. Additionally, shifts in absorption maxima suggest that the extracts induce different degrees of perturbation in the local environment of peptide bonds. These effects could be mediated by hydrophobic interactions, hydrogen bond formation, or alterations in the conformational equilibrium between α-helix and β-sheets.[11,12,27–29,50–55]

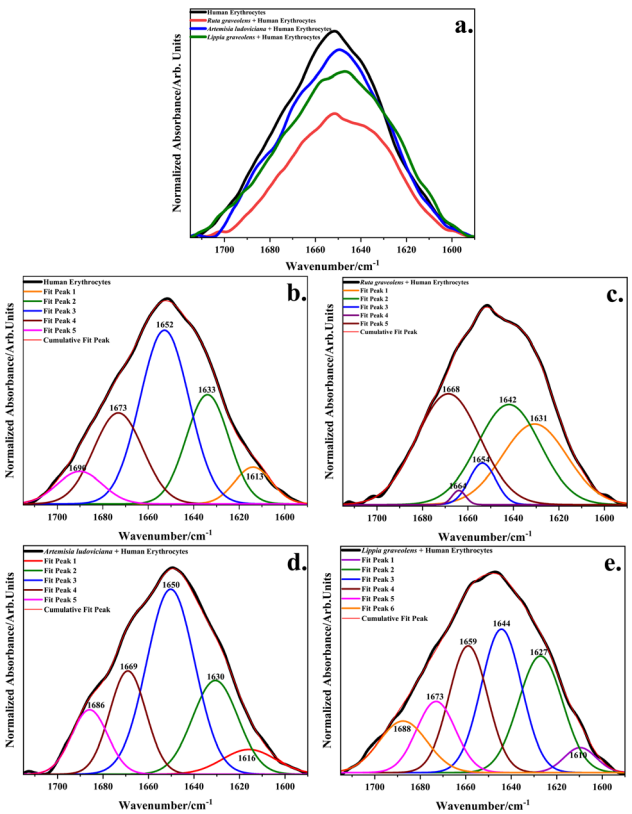

Fig. 5 ATR-FTIR spectra (1700–1600 cm^{-1}) of: (a) human erythrocytes and human erythrocytes treated with ethanolic extracts of *Ruta graveolens*, *Artemisia ludoviciana*, and *Lippia graveolens*, and (b–e) spectral deconvolution of each sample.

In Fig. 5(b), the spectral deconvolution of untreated erythrocytes is shown, where five bands centred at 1690 cm^{-1}, 1673 cm^{-1}, 1652 cm^{-1}, 1633 cm^{-1}, and 1613 cm^{-1} are observed. In proteins in the native state with predominance of α-helix structures, such as haemoglobin and various integral and peripheral membrane proteins present in human erythrocytes, the absorption band of α-helix structures typically appears between 1660–1650 cm^{-1}, the absorption band associated with β-sheet structures is found between 1640–1610 cm^{-1} and between 1690–1680 cm^{-1} those corresponding to antiparallel β-sheet structures, whilst β-turns are found between 1680–1670 cm^{-1}. In the spectral deconvolution, an intense band centred at 1652 cm^{-1} corresponds to secondary structures with α-helix conformation. Likewise, the bands centred at 1673 cm^{-1} and 1633 cm^{-1} are due to the presence of β-turns and β-sheet, respectively. On the other hand, the bands centred at 1690 cm^{-1} and 1613 cm^{-1} correspond to β-sheet type structures. This spectral profile is associated with the native state of erythrocyte membrane proteins, presenting a balanced structural distribution among the different elements of protein secondary conformation.[11,12,27–29,50–55]

Fig. 5(c) presents the spectral deconvolution of human erythrocytes treated with the ethanolic extract of *Ruta graveolens*, where five bands centred at 1668, 1664, 1654, 1642, and 1631 cm^{-1} are observed. The band centred at 1652 cm^{-1} of the control spectrum associated with α-helix structures undergoes a shift toward 1654 cm^{-1} and a significant decrease in the intensity, which suggests a loss of α-helix structures. Likewise, an increase in the intensity of the bands centred at 1642 cm^{-1} and 1631 cm^{-1} is observed, which indicates an enrichment in β-sheet type secondary structures. The band centred at 1668 cm^{-1} presents an increase in its intensity, which reflects a greater proportion of β-turns. All the above suggest a conformational transition induced by interaction with secondary metabolites present in the extract, probably through α-helix destabilization mechanisms and subsequent reorganisation toward β-structures. The presence of bioactive compounds such as flavonoids and coumarins in *Ruta graveolens* could favour this effect through specific interactions with the carbonyls of the peptide backbone, promoting the formation of ordered aggregates that alter the native structure of membrane proteins.[11,12,27–29,50–55]

Fig. 5(d) shows the spectral deconvolution of human erythrocytes treated with the ethanolic extract of *Artemisia ludoviciana*, where five bands centred at 1686, 1669, 1650, 1630, and 1616 cm^{-1} are observed. The band centred at 1650 cm^{-1} suggests partial conservation of α-helix type secondary structures, while the band centred at 1630 cm^{-1} indicates the presence of β-sheet type structures. The appearance of the band centred at 1686 cm^{-1} is associated with an increase in antiparallel β-sheet type conformations, which evidences a significant reorganisation of the conformational pattern of membrane proteins. This spectral profile suggests that *Artemisia ludoviciana* induces selective structural modification through

molecular interactions between bioactive metabolites present in the extract, such as sesquiterpene lactones and flavonoids, as well as with polar or charged residues of membrane proteins. Such interactions, probably of polar nature or through hydrogen bond formation, could favour the transition from structurally ordered domains toward configurations of greater energetic stability, potentially affecting protein functionality in the context of the lipid bilayer.[11,12,27–29,50–55]

Finally, Fig. 5(e) shows the spectral deconvolution corresponding to human erythrocytes treated with the ethanolic extract of *Lippia graveolens*, where six bands centred at 1688, 1673, 1659, 1644, 1627, and 1610 cm^{-1} are observed. The band centred at 1644 cm^{-1} indicates an increase in the proportion of β-sheet type secondary structures, while the band located at 1627 cm^{-1} suggests the presence of more intense intermolecular interactions or the adoption of less dynamic conformations, characteristics frequently associated with protein aggregation phenomena. These conformational changes could be mediated by the action of phenolic compounds such as carvacrol and thymol, bioactive metabolites present in *Lippia graveolens*, which are known for their ability to interact with aromatic residues and carbonyl groups of the peptide backbone. Such interactions can limit the conformational flexibility of proteins or induce a structural reorganisation toward partially collapsed states, which could alter the functional dynamics of membrane proteins.[11,12,27–29,50–55]

3.3.4 Spectral region from 1600 cm^{-1} to 1450 cm^{-1}. The amide II region provides information about the secondary conformation of proteins, as well as about the intra- and intermolecular interactions that stabilize their structure. This band originates mainly from the bending vibration of the N–H group coupled to the stretching vibration of the C–N bond of the peptide backbone. Due to its sensitivity to variations in the molecular environment, amide II acts as an effective spectroscopic indicator to detect structural alterations induced by physicochemical factors, such as changes in medium polarity, oxidative stress, or interactions with bioactive metabolites. These modifications can reflect denaturation processes, conformational reorganisation, or the formation of new intermolecular bonds with membrane proteins.

In Fig. 6(a), the ATR-FTIR spectra of untreated human erythrocytes and those treated with ethanolic extracts of *Ruta graveolens*, *Artemisia ludoviciana*, and *Lippia graveolens* are shown in the amide II spectral region. In most cases, modifications in the spectral profile are observed when compared to the control spectrum. These changes are appreciated in the abundant appearance of shoulders, as well as in the increase and decrease in intensity; these spectral modifications can be attributed to the interactions that occur with the secondary metabolites present in the plant extracts.[11,12,27–29,50–55]

Fig. 6(b) shows the spectral deconvolution of untreated human erythrocytes, where six bands centred at 1569, 1544, 1536, 1528, 1515, and 1500 cm^{-1} are observed. The band centred at 1544 cm^{-1} is attributed to α-helix type structures since these structures are typically found between 1550–1540 cm^{-1}, while secondary structures with β-sheet conformation are usually located between 1540–1520 cm^{-1}, which indicated that

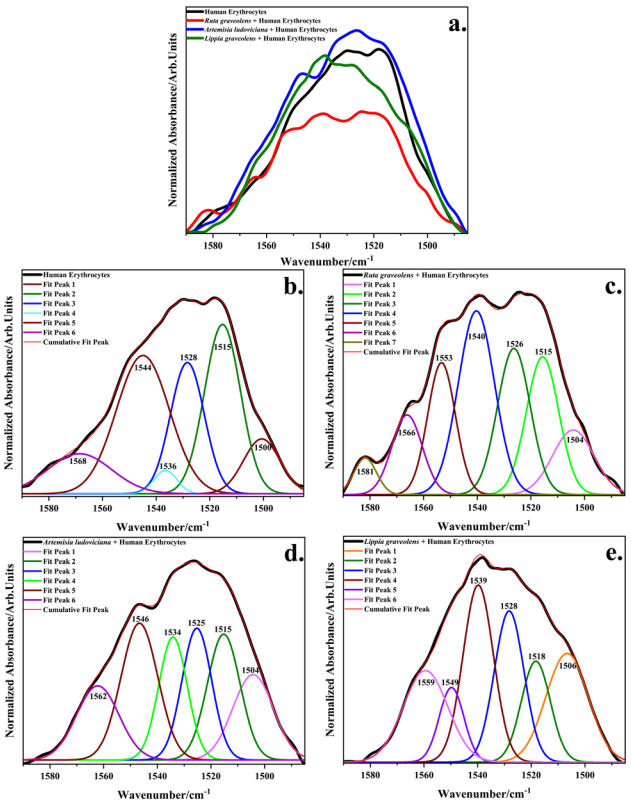

Fig. 6 ATR-FTIR spectra (1600–1450 cm^{-1}) of: (a) human erythrocytes and human erythrocytes treated with ethanolic extracts of *Ruta graveolens*, *Artemisia ludoviciana*, and *Lippia graveolens*, and (b–e) spectral deconvolution of each sample.

bands centred at 1536 cm^{-1} and 1528 cm^{-1} correspond to β-sheet secondary structures, on the other hand, the band centred at 1568 cm^{-1} correspond to β-turn type structures. The band centred at 1500 cm^{-1} is due to CH_2 and CH_3 deformation of lipids and proteins. The symmetry, resolution, and relative distribution of the bands indicate an organisation and stable protein environment, characteristic of erythrocyte membranes in the native state.[11,12,27–29,50–55]

On the other hand, exposure of human erythrocytes to the ethanolic extract of *Ruta graveolens* induced modifications in the spectral profile of amide II, changes that are observed in the general decrease in intensity and in the presence of various shoulders. In the spectral deconvolution of Fig. 6(c), seven bands centred at 1581, 1655, 1553, 1540, 1526, 1515, and 1504 cm^{-1} are observed, which indicates a significant redistribution of protein conformational content when compared to the control. In particular, the control spectrum band centred at 1544 cm^{-1} undergoes a shift toward 15 540 cm^{-1}, indicating a conformational change from α-helix to β-sheets. The bands centred at 1566 cm^{-1} and 1581 cm^{-1} indicate a conformational increase of β-turns, which reflects specific interactions with peptide groups. This spectral behaviour with a greater abundance of β-structures suggests a very pronounced structural disorganisation, due to the action of bioactive metabolites present in *Ruta graveolens*, such as furocoumarins, flavonoids, and alkaloids, which could affect both

intramolecular interactions and the anchoring of proteins to the lipid bilayer.[11,12,27–29,50–55]

Fig. 6(d) shows the spectral deconvolution of human erythrocytes treated with the ethanolic extract of *Artemisia ludoviciana*, in which six bands centred at 1562, 1546, 1534, 1525, 1515, and 1504 cm^{-1} are observed. The proximity of these bands to those observed in untreated erythrocytes suggests that the secondary structure of proteins in mostly conserved. The slight shift toward 1534 cm^{-1} of the control spectrum, along with the stability of the bands centred at 1515 cm^{-1} and 1504 cm^{-1}, indicate that the bioactive metabolites present in *Artemisia ludoviciana* exert a modulating, rather that disruptive, effect on protein structure. This spectral behaviour suggests that interactions between compounds in the extract, possibly flavonoids, sesquiterpene lactones, or other polar phenols, and membrane proteins occur preferentially at the surface level, through non-covalent interactions such as hydrogen bonds or dipole–dipole interactions, without inducing significant modifications in the secondary conformation of proteins.[11,12,27–29,50–55]

Finally, the spectral deconvolution of human erythrocytes treated with the ethanolic extract of *Lippia graveolens* is shown in Fig. 6(e), and six bands centred at 1559, 1549, 1539, 1528, 1518, and 1506 cm^{-1} are observed. The presence of intense bands centred at 1539 cm^{-1}, 1528 cm^{-1}, and 1518 cm^{-1} may be related to partial fragmentation of the β-sheet type secondary structure of membrane proteins, while the bands centred at 1559 cm^{-1} and 1549 cm^{-1} could be associated with polar interactions with specific domains. However, β-structures predominate. This complexity in the spectral profile can be related to the phytochemical richness of *Lippia graveolens*, capable of interacting with carbonyl and aromatic residues of the peptide backbone. The combined action of these metabolites seems to induce a partial reorganisation of the internal bonds of proteins, promoting a more dynamic and less compact conformational environment.[11,12,27–29,50–55]

Taken together, the ATR-FTIR analyses and spectral deconvolution demonstrate that ethanolic extracts of *Ruta graveolens*, *Artemisia ludoviciana*, and *Lippia graveolens* induce structural alterations on human erythrocytes, affecting both lipid organisation of the membrane and the secondary conformation of their proteins. The shifts and variations in the characteristic regions of the methylene and carbonyl groups suggests changes in the fluidity, rigidity and packing of the bilayer, whilst the modifications in the amide I and II bands reflect a possible protein reorganisation, with a tendency towards partial destabilisation. These observations indicate that the spectroscopic response result from a combined contribution between the secondary metabolites of the extracts and the cellular structures, which suggests that, in addition to the predominance of the erythrocytic signal, there exists a modulatory effect derived from the direct interaction of the bioactive compounds with the membrane and surface proteins.

4. Conclusions

ATR-FTIR spectroscopy, together with spectral deconvolution analysis, showed that ethanolic extracts of *Ruta graveolens*, *Artemisia ludoviciana*, and *Lippia graveolens* induce specific structural modifications on human erythrocyte membranes, reflecting differentiated interactions according to their phytochemical profiles. The bioactive secondary metabolites present, such as monoterpenes, flavonoids, sesquiterpene lactones, phenolic compounds, *etc.*, selectively interact with the lipid bilayer, with membrane proteins and phosphate groups, modulating molecular organisation. ATR-FTIR spectra showed that *Ruta graveolens* induces the greatest lipid disorganisation and protein conformational alterations, followed by *Artemisia ludoviciana* and *Lippia graveolens*. Transitions from secondary structures with α-helix conformation toward β-sheet type secondary structures were observed, which provides evidence of the type of interactions being generated: hydrogen bonds, dipole–dipole, van der Waals, *etc.*, between the secondary metabolites with the lipid bilayer and with the proteins. These results provide biophysical evidence on the capacity of plant extracts to modulate cellular components.

Author contributions

Emmanuel de la O-Cuevas: investigation, methodology, conceptualization, formal analysis, writing original draft; P. Gallegos-Flores: writing-review & editing; J. J. Ortega-Sigala: writing-review & editing; H. Tototzintle-Huitle: writing-review & editing; José M. Saniger: conceptualization, review & editing; E. L. Esparza-Ibarra: conceptualization, resource, writing-review & editing.

Conflicts of interest

There are not conflicts to declare.

Data availability

The datasets generated and/or analyzed during this study are available upon reasonable request from the lead authors: Dr Edgar León Esparza Ibarra (lesparza@uaz.edu.mx) and Dr Emmanuel de la O Cuevas (emmanuel.delao@fisica.uaz.edu.mx).

Supplementary information: positive control for cell lysis. See DOI: **https://doi.org/10.1039/d5ra06459g**.

Acknowledgements

E. O. C. wishes to acknowledge financial support from SECIHTI, México, for a postdoctoral fellowship.

References

1 World Health Organization, *Traditional Medicine Has A Long History Of Contributing To Conventional Medicine And Continues To Hold Promise*, WHO, 2023, **https://www.who.int/news-room/feature-stories/detail/traditional-medicine-has-a-long-history-of-contributing-to-conventional-medicine-and-continues-to-hold-promise**.

2 World Health Organization, *Integrating Traditional Medicine in Health Care, WHO Southeast Asia*, 2023. **https://**

www.who.int/southeastasia/news/feature-stories/detail/integrating-traditional-medicine.
3 World Health Organization, *WHO Establishes the Global Centre for Traditional Medicine in India*, WHO, 2022. https://www.who.int/news/item/25-03-2022-who-establishes-the-global-centre-for-traditional-medicine-in-india.
4 A. G. Atanasov, S. B. Zotchev, V. M. Dirsch and C. T. Supuran, Natural products in drug discovery: advances and opportunities, *Nat. Rev. Drug Discovery*, 2021, **20**(3), 200–216.
5 N. Nasim, I. S. Sandeep and S. Mohanty, Plant-derived natural products for drug discovery: current approaches and prospects, *Nucleus*, 2022, **65**(3), 399–411.
6 M. J. Rodrigues, Bioprospecting of Natural Products from Medicinal Plants, *Plants*, 2024, **13**(24), 3556.
7 I. Dincheva, I. Badjakov and B. Galunska, New Insights in the Research on Bioactive Compounds from Plant Origins with Nutraceutical and Pharmaceutical Potential II, *Plants*, 2025, **14**(4), 500.
8 M. Cupido, J. A. De-Nova and V. G. Cilia-López, Aproximaciones evolutivas en etnobotánica de plantas medicinales y bioprospección, *Bot. Sci.*, 2024, **102**(1), 26–38.
9 E. L. Menéndez, Medicina tradicional mexicana: los objetivos y las formas de estudiarla relaciones, *Estudios de historia y sociedad*, 2023, **44**(174), 149–171.
10 S. I. C. Martínez, N. A. S. López, J. C. Medina and Y. M. Paredes, La medicina tradicional: perspectiva turística y patrimonial, *Dictamen Libre*, 2023, (33), 105–117.
11 R. Bañuelos-Valenzuela, L. Delgadillo-Ruiz, F. Echavarría-Cháirez, O. Delgadillo-Ruiz and C. Meza-López, Chemical composition and FTIR of ethane extracts of *Larrea tridentata*, *Origanum vulgare*, *Artemisa ludoviciana* and *Ruta graveolens*, *Agrociencia*, 2018, **52**(3), 309–321.
12 L. Delgadillo Ruíz, R. Bañuelos Valenzuela, O. Delgadillo Ruíz, M. Silva Vega and P. Gallegos Flores, Composición química y efecto antibacteriano *in vitro* de extractos de *Larrea tridentata*, *Origanum vulgare*, *Artemisa ludoviciana* y *Ruta graveolens*, *Nova scientia*, 2017, **9**(19), 273–290.
13 T. Hernández, A. M. García-Bores, R. Serrano, G. Ávila, P. Dávila, H. Cervantes and R. Lira, Fitoquímica y actividades biológicas de plantas de importancia en la medicina tradicional del Valle de Tehuacán-Cuicatlán, *Tip. Rev. Espec. Ciencias Químico-Biol.*, 2015, **18**(2), 116–121.
14 C. G. Luján, A. Martínez, J. L. Ortega and F. Castro, Componentes químicos y su relación con las actividades biológicas de algunos extractos vegetales, *QuimicaViva*, 2010, **9**(2), 86–96.
15 C. C. Arcila-Lozano, G. Loarca-Piña, S. Lecona-Uribe and E. González de Mejía, El orégano: propiedades, composición y actividad biológica de sus componentes, *Arch. Latinoam. Nutr.*, 2004, **54**(1), 100–111.
16 M. P. Barrón González, A. E. Medrano Cosme, K. I. Leal López, D. J. Eguiarte Lara, F. L. Cuellar Guevara, Y. Quiñones Gutiérrez and R. G. Rodríguez Garza, Actividad anti- helicobacter pylori del extracto metanólico de Artemisia ludoviciana, *Investigación y Desarrollo en Ciencia y Tecnología de Alimentos*, 2019, **4**, 284–294.
17 J. H. Elizondo-Luevano, R. Quintanilla-Licea, S. L. Castillo-Hernández, E. Sánchez-García, M. Bautista-Villarreal, G. M. González-Meza and M. Kačániová, *In vitro* evaluation of anti-hemolytic and cytotoxic effects of traditional Mexican medicinal plant extracts on human erythrocytes and cell cultures, *Life*, 2024, **14**(9), 1176.
18 E. C. F. Júnior, B. P. Costa, J. C. P. Freire, W. O. de Sousa Melo, H. de Luna Freire Pessôa, D. Q. de Castro Gomes and J. V. Pereira, Use of erythrocytes in cytotoxicity and toxicity assays of medicinal plant extracts: analysis of their application and bibliometric study, *Bol. Latinoam. Caribe Plantas Med. Aromat.*, 2019, **18**(4), 359–377.
19 O. G. Shevchenko, Blood erythrocytes—a biological model for evaluating antioxidant activity of chemical compounds (a review), *Russ. J. Bioorg. Chem.*, 2024, **50**(6), 2191–2208.
20 S. Malehmir, M. A. Esmaili, M. Khaksary Mahabady, A. Sobhani-Nasab, A. Atapour, M. R. Ganjali and A. Moradi Hasan-Abad, A review: hemocompatibility of magnetic nanoparticles and their regenerative medicine, cancer therapy, drug delivery, and bioimaging applications, *Front. Chem.*, 2023, **11**, 1249134.
21 S. Himbert and M. C. Rheinstädter, Structural and mechanical properties of the red blood cell's cytoplasmic membrane seen through the lens of biophysics, *Front. Physiol.*, 2022, **13**, 953257.
22 E. Lindbergh, *Hemolytic Anemia in Disorders of Red Cell Metabolism*, Springer Science & Business Media, 2012.
23 G. Barshtein, Biochemical and biophysical properties of red blood cells in disease, *Biomolecules*, 2022, **12**(7), 923.
24 M. Al-Kelani and N. Buthelezi, Advancements in medical research: exploring Fourier Transform Infrared (FTIR) spectroscopy for tissue, cell, and hair sample analysis, *Skin Res. Technol.*, 2024, **30**(6), e13733.
25 S. Jain, A. Thomas, G. Y. Zhuo and N. Mazumder, Fourier Transform Infrared (FTIR) Spectroscopy of Biomolecules, *Recent Advances in Infrared Spectroscopy and Its Applications in Biotechnology*, 2025, p. 101.
26 A. C. S. Talari, M. A. G. Martinez, Z. Movasaghi, S. Rehman and I. U. Rehman, Advances in Fourier transform infrared (FTIR) spectroscopy of biological tissues, *Appl. Spectrosc. Rev.*, 2017, **52**(5), 456–506.
27 S. A. Tatulian, Analysis of protein–protein and protein–membrane interactions by isotope-edited infrared spectroscopy, *Phys. Chem. Chem. Phys.*, 2024, **26**(33), 21930–21953.
28 S. A. Tatulian, FTIR analysis of proteins and protein–membrane interactions, in *Lipid-protein Interactions: Methods and Protocols*, Springer, 2019, pp. 281–325.
29 S. A. Tatulian, Structural characterization of membrane proteins and peptides by FTIR and ATR-FTIR spectroscopy, in *Lipid–protein Interactions: Methods and Protocols*, Humana press, 2012, pp. 177–218.
30 P. Lasch, Spectral pre-processing for biomedical vibrational spectroscopy and microspectroscopic imaging, *Chemom. Intell. Lab. Syst.*, 2012, **117**, 100–114.
31 M. Asemani and A. R. Rabbani, Detailed FTIR spectroscopy characterization of crude oil extracted asphaltenes: Curve

resolve of overlapping bands, *J. Petrol. Sci. Eng.*, 2020, **185**, 106618.

32 C. Kyomugasho, S. Christiaens, A. Shpigelman, A. M. Van Loey and M. E. Hendrickx, FT-IR spectroscopy, a reliable method for routine analysis of the degree of methylesterification of pectin in different fruit-and vegetable-based matrices, *Food Chem.*, 2015, **176**, 82–90.

33 G. I. Dovbeshko, N. Y. Gridina, E. B. Kruglova and O. P. Pashchuk, FTIR spectroscopy studies of nucleic acid damage, *Talanta*, 2000, **53**(1), 233–246.

34 J. A. Pierce, R. S. Jackson, K. W. Van Every, P. R. Griffiths and H. Gao, Combined deconvolution and curve fitting for quantitative analysis of unresolved spectral bands, *Anal. Chem.*, 1990, **62**(5), 477–484.

35 D. M. Byler and H. Susi, Examination of the secondary structure of proteins by deconvolved FTIR spectra, *Biopolymers: Original Research on Biomolecules*, 1986, **25**(3), 469–487.

36 H. Susi, D. M. Byler and J. M. Purcell, Estimation of β-structure content of proteins by means of deconvolved FTIR spectra, *J. Biochem. Biophys. Methods*, 1985, **11**(4–5), 235–240.

37 D. M. Byler, and H. Susi. *Protein structure by FTIR self-deconvolution. In Fourier and Computerized Infrared Spectroscopy*, 1985, vol. 553, pp. 289–290.

38 C. D. Grande Tovar, J. I. Castro, C. H. Valencia Llan, D. P. Navia Porras, J. Delgado Ospina, M. E. Valencia Zapata and M. N. Chaur, Synthesis, characterization, and histological evaluation of chitosan-*Ruta graveolens* essential oil films, *Molecules*, 2020, **25**(7), 1688.

39 J. Sivakamavalli, O. Deepa and B. Vaseeharan, Discrete nanoparticles of *Ruta graveolens* induces the bacterial and fungal biofilm inhibition, *Cell Commun. Adhes.*, 2014, **21**(4), 229–238.

40 W. Daoudi, B. Bouhout, M. Azzouzi, A. Ibn Mansour and A. Oussaid, Biological activity of leaves and stems extracts of *Artemisia herba*-alba from the Oriental region of Morocco and extraction of cellulose from this plant (isolation, modification and applications), *Moroccan J. Chem.*, 2022, **10**(4), 622–638.

41 N. Barbieri, A. Sanchez-Contreras, A. Canto, J. V. Cauich-Rodriguez, R. Vargas-Coronado and L. M. Calvo-Irabien, Effect of cyclodextrins and Mexican oregano (*Lippia graveolens* Kunth) chemotypes on the microencapsulation of essential oil, *Ind. Crops Prod.*, 2018, **121**, 114–123.

42 K. M. Soto, M. Hernández-Iturriaga, A. Cárdenas and S. Mendoza, Biosynthesis of silver nanoparticles mediated by *Lippia graveolens* aqueous extract, *J. Mex. Chem. Soc.*, 2024, **68**(3), 402–411.

43 K. Z. Liu, M. H. Shi and H. H. Mantsch, Molecular and chemical characterization of blood cells by infrared spectroscopy: a new optical tool in hematology, *Blood Cells, Mol., Dis.*, 2005, **35**(3), 404–412.

44 A. Fadlelmoula, D. Pinho, V. H. Carvalho, S. O. Catarino and G. Minas, Fourier transform infrared (FTIR) spectroscopy to analyse human blood over the last 20 years: a review towards lab-on-a-chip devices, *Micromachines*, 2022, **13**(2), 187.

45 A. Blat, J. Dybas, M. Kaczmarska, K. Chrabaszcz, K. Bulat, R. B. Kostogrys and K. M. Marzec, An analysis of isolated and intact rbc membranes—A comparison of a semiquantitative approach by means of FTIR, nano-FTIR, and Raman spectroscopies, *Anal. Chem.*, 2019, **91**(15), 9867–9874.

46 H. Liu, Q. Su, D. Sheng, W. Zheng and X. Wang, Comparison of red blood cells from gastric cancer patients and healthy persons using FTIR spectroscopy, *J. Mol. Struct.*, 2017, **1130**, 33–37.

47 F. S. Ruggeri, C. Marcott, S. Dinarelli, G. Longo, M. Girasole, G. Dietler and T. P. Knowles, Identification of oxidative stress in red blood cells with nanoscale chemical resolution by infrared nanospectroscopy, *Int. J. Mol. Sci.*, 2018, **19**(9), 2582.

48 E. Szczesny-Malysiak, J. Dybas, A. Blat, K. Bulat, K. Kus, M. Kaczmarska and K. M. Marzec, Irreversible alterations in the hemoglobin structure affect oxygen binding in human packed red blood cells, *Biochim. Biophys. Acta, Mol. Cell Res.*, 2020, **1867**(11), 118803.

49 V. Tucureanu, A. Matei and A. M. Avram, FTIR spectroscopy for carbon family study, *Crit. Rev. Anal. Chem.*, 2016, **46**(6), 502–520.

50 M. Jackson and H. H. Mantsch, The use and misuse of FTIR spectroscopy in the determination of protein structure, *Crit. Rev. Biochem. Mol. Biol.*, 1995, **30**(2), 95–120.

51 J. Kong and S. Yu, Fourier transform infrared spectroscopic analysis of protein secondary structures, *Acta Biochim. Biophys. Sin.*, 2007, **39**(8), 549–559.

52 B. Shivu, S. Seshadri, J. Li, K. A. Oberg, V. N. Uversky and A. L. Fink, Distinct β-sheet structure in protein aggregates determined by ATR-FTIR spectroscopy, *Biochemistry*, 2013, **52**(31), 5176–5183.

53 J. De Meutter and E. Goormaghtigh, Amino acid side chain contribution to protein FTIR spectra: impact on secondary structure evaluation, *Eur. Biophys. J.*, 2021, **50**(3), 641–651.

54 J. De Meutter and E. Goormaghtigh, Evaluation of protein secondary structure from FTIR spectra improved after partial deuteration, *Eur. Biophys. J.*, 2021, **50**(3), 613–628.

55 J. De Meutter and E. Goormaghtigh, Protein structural denaturation evaluated by MCR-ALS of protein microarray FTIR spectra, *Anal. Chem.*, 2021, **93**(40), 13441–13449.